Hydrodynamics of Disturbed Flow and Erosion–Corrosion. Part II — Two-phase Flow Study

S. NEŠIĆ and J. POSTLETHWAITE

Department of Chemical Engineering, University of Saskatchewan, Saskatoon, SK S7N 0W0

Erosion–Corrosion in turbulent, two-phase liquid/particle flow with recirculation, after a sudden pipe expansion is studied by the application of a numerical flow model along with two different erosion models. The flow model, which is based on a two-phase flow version of a standard two-equation model of turbulence and a stochastic simulation of particle-fluid turbulence interactions, is capable of successfully predicting local values of time averaged fluid velocities and turbulent fluctuations, as well as predicting particle dispersion and particle-wall interaction. The erosion models used are that of Finnie (1960) and a modified version suggested by Bergevin (1984).

The agreement of the predicted and measured hydrodynamic parameters, for flow through a sudden expansion, was satisfactory. Predictions of erosion rates using Bergevin's modified model were in good agreement with the stainless steel erosion measurements for a 2% water/sand slurry flow. The erosion–corrosion model was successful in predicting the overall pattern and rates of metal loss for carbon steel.

On a étudié le phénomène «érosion–corrosion» dans un écoulement turbulent biphasique liquide/particules en recirculation après une expansion abrupte du tuyau, à l'aide d'un modèle d'écoulement numérique et de deux modèles d'érosion différents. Le modèle d'écoulement, qui est basé sur une version d'écoulement biphasique d'un modèle de turbulence à deux équations standard et une simulation stochastique d'interactions de turbulence particles-fluides, est capable de prédire avec succès (1) les valeurs des débits moyens par rapport au temps et les fluctuations turbulentes et (2) la dispersion des particules et l'interaction particules-paroi. Les modèles d'érosion utilisés sont ceux de Finnie (1960) et une version modifiée suggérée par Bergevin (1984).

L'accord des paramètres hydrodynamiques prédits et mesurés pour un écoulement avec une expansion abrupte, est satisfaisant. Les prédictions des vitesses d'érosion avec le modèle modifié de Bergevin montrent un bon accord avec les mesures d'érosion de l'acier inoxydable pour un écoulement d'eau/boues sablonneuses à 2%. Le modèle d'érosion et de corrosion prédit avec succès le modèle général et les vitesses de la perte de métal pour l'acier au carbone.

Keywords: erosion–corrosion, liquid/solid flow model, slurry flow, two-equation turbulence model.

Modelling of erosion–corrosion processes is undertaken to further our understanding of corrosion mechanisms at the fundamental level by comparing the results of the modelling with experimental data, with a longer term objective of producing predictive models which could be incorporated into expert systems.

Oxygen-mass transfer controlled erosion–corrosion in straight slurry pipelines can be modelled by the application of appropriate mass transfer correlations which relate the Sherwood, Schmidt and Reynolds numbers (Postlethwaite et al., 1986). This simple approach cannot be applied to erosion–corrosion in many practical situations, where the metal loss occurs under conditions of disturbed flow at geometrical irregularities such as weld beads and fittings, when the flow separates and/or impinges on the walls (Glaeser, 1982). A knowledge of the local flow structure along with details of particle-wall interactions is required in order to model such erosion–corrosion (Zeisel and Durst, 1990).

This paper describes the application of a model for predicting the flow structure and the erosion and corrosion rates, to the results of recent experimental erosion and erosion–corrosion studies, at a sudden expansion in a pipe.

Liquid/Particle flow model

The turbulent fluid flow field was modelled by a well established Eulerian based, control volume procedure, for solution of time averaged flow equations. The motion of a dispersed particulate phase can be determined by either Eulerian or Lagrangian methods, depending on whether particles are treated as a "second fluid" (Pourahmadi and Humphrey, 1983), or a large number of representative trajectories are calculated in the flow domain (Milojević et al., 1986). According to a numerical study by Durst et al. (1984), both methods have their advantages, but for the case of particle size distributions and significant particle-wall interactions, the Lagrangian approach seems advantageous, since it gives more direct information about the particles.

The following assumptions were made:

- Particles are treated as sources or sinks of momentum, mass and energy in the fluid;
- Particles have a negligibly small volume compared to the total volume of the flow;
- Direct particle–particle interactions are negligible, but fluid-particle interactions lead to a two-way coupling;
- External fluxes and stresses act directly on the fluid only;
- Brownian movement of the particles or movement due to pressure gradients and particle rotation is neglected;
- Particles are spherical.

The present fluid flow model is based on a standard two-equation, kinetic energy of turbulence — rate of turbulent dissipation ($k - \epsilon$) model of turbulence described by Launder and Spalding (1974). Equations for mass, momentum, kinetic energy of turbulence and its rate of dissipation were solved for the case of axis-symmetrical flow (full equations given elsewhere by Nešić and Postlethwaite, 1990).

The motion of particles in fluid turbulence is predicted by means of the Lagrangian Stochastic–Deterministic model (LSD), proposed by Milojević et al. (1986). Particle flow properties are calculated by taking ensemble averages from a large number of particle trajectories for the same control volumes as for the fluid phase. Individual particle trajectories from the inlet to the outlet of the flow domain are calculated by numerical solution of "instantaneous" particle momentum equation.

$$m^p \, d\vec{V}^p/dt = [\rho \, C_D \, A^p (\vec{V} - \vec{V}^p) | \vec{V} - \vec{V}^p | / 2] + \vec{F} \quad (1)$$

The numerical solution of fluid flow equations provides the fields of mean velocity components and kinetic energy of turbulence $\mathbf{k}$ and its rate of dissipation ϵ. Knowing local $\mathbf{k}$ and ϵ values, it is possible to estimate turbulence time and length scales, corresponding to the large, energy containing eddies. The particle Equation (1) is made "instantaneous" (stochastic) by generating a random fluid velocity field around the particle ($\vec{v}$) on the basis of known turbulence energy and time and length scales. Fluid velocity fluctuations (u, v, w) are generated independently as random numbers from a Gaussian distribution with a mean of zero and a standard deviation (u', v', w'), which can be determined from the local value of kinetic energy of turbulence:

$$u' = v' = w' = (2\mathbf{k}/3)^{0.5} \quad \ldots\ldots (2)$$

The fluctuating components of fluid velocity (u, v, w) are then added to the determined mean fluid velocity components (U, V, W) to obtain the "instantaneous" values of fluid velocity ($\tilde{u}$, $\tilde{v}$, $\tilde{w}$) which are needed in the Equation (1) for particle motion. The fluid instantaneous velocity components ($\tilde{u}$, $\tilde{v}$, $\tilde{w}$) are kept constant until the local Lagrangian integral time scale T_L expires, which corresponds to the "lifetime" of large eddies. T_L can be estimated from local values of kinetic energy of turbulence and its rate of dissipation:

$$T_L = 0.3\mathbf{k}/\epsilon \quad \ldots\ldots (3)$$

The "size" of an eddy estimated from local length scale of turbulence L_L is:

$$L_L = u' T_L \quad \ldots\ldots (4)$$

This model enables direct accounting for the relative motion between the eddy and the particles, hence enables determination of the effect of crossing trajectories. Particle-eddy interaction is stopped when either the eddy lifetime is over, or when a particle crosses the eddy. Then a new fluctuation velocity component is generated.

Boundary conditions for the particles have to be defined on the inlet, on the walls and the axis. The inlet particle velocity can be given or assumed known from experiments. On the walls and the axis, a model of simple reflection is used:

$$\tilde{u}_R^p = \psi_R \tilde{u}^p \quad \ldots\ldots (5)$$

where

$$\psi_R = \begin{cases} 0 - 1 & \text{on the wall} \\ 1 & \text{on the axis} \end{cases} \quad \ldots\ldots (6)$$

The solution procedure has the following steps:

1. solution of the fluid (single-phase) flow equations until a reasonably converged solution is obtained;
2. calculation of the particle trajectories and particle source terms for the fluid flow equations;
3. solution of the fluid flow equations with new source terms;
4. check for convergence, if not reached go to step 2;
5. final calculations and printout.

Erosion model

Erosion of steel by sand particles was initially modelled by using the "cutting wear" approach of Finnie (1960).

$$Q \approx cm^p (U^p)^2 (\sin 2\alpha - 3 \sin^2 \alpha)/4p \quad \text{for } \alpha \leq 18.5° \quad \ldots\ldots (7)$$

$$Q \approx cm^p (U^p)^2 \cos^2 \alpha / 12p \quad \text{for } \alpha \geq 18.5° \quad \ldots\ldots (8)$$

However, it was shown recently by Zeisel and Durst (1990) that these equations are not suitable for impact angles above 45°. They suggested that at higher angles, erosion rates obtained from Finnie's Equations (7) and (8) should be increased to take into account the "destruction" process at angles close to 90°. Further, Finnie's Equations (7) and (8) contain an arbitrary constant, c, that takes into account the proportion of the particles which impact on the surface, that do the damage. Finnie (1960) suggested that this constant could be $c \approx 0.5$.

Another approach is the one suggested by Bergevin (1984): we can assume that only the particles that have the normal impact velocity ($U^p \sin \alpha$) greater than some critical value for the given material, U_{cr}, create plastic deformation and erosion. This is in accordance with the findings of Bitter (1963), that particles impacting with a velocity lower than the critical, will create only non-destructive elastic deformation. Accordingly, Finnie's Equations (7) and (8) were modified by inserting ($U^p \sin \alpha - U_{cr}$) instead of $U^p \sin \alpha$.

$$Q \approx m^p (U^p \sin \alpha - U_{cr}) [U^p \cos \alpha - 3(U^p \sin \alpha - U_{cr})/2]/2p \quad \text{for } \alpha \leq 18.5° \quad \ldots\ldots (9)$$

$$Q \approx m^p (U^p \sin \alpha - U_{cr})^2 \cos^2 \alpha / (12p \sin^2 \alpha) \quad \text{for } \alpha \geq 18.5° \quad \ldots\ldots (10)$$

The critical velocity for plastic deformation U_{cr} was determined by Bitter (1963) for a number of different materials.

Results and discussion

When modelling erosion–corrosion in disturbed two-phase flow systems, three main aspects of the problem have to be studied: the structure of the liquid/particle flow, the erosion component and the corrosion component of metal loss. Models used for the flow and the erosion are described above. Postlethwaite et al. (1986) have shown that the erosion–corrosion in straight slurry pipelines is oxygen-mass transfer controlled. Mass transfer was not directly modelled and results obtained in the single-phase study (Nešić and Postlethwaite, Part I, 1991) are used to explain some of the corrosion aspects of the results.

Most severe erosion–corrosion damage occurs under disturbed flow conditions when flow separation, reattachment and recirculation are present. This creates higher mass transfer rates and corrosion, and when solids are present, an increase in particle wall impacts and erosion. Flow of a liquid/solid mixture through a sudden pipe expansion, was selected as model situation for disturbed flow conditions, with sufficient complexity and practical importance.

To verify the accuracy of the model, three test cases were selected: hydrodynamic measurements of a liquid/particle flow through a sudden expansion, by Blatt et al. (1989), the stainless steel erosion measurements for a similar geometry, by Lotz and Postlethwaite (1990) and the mild steel erosion–corrosion measurements made by

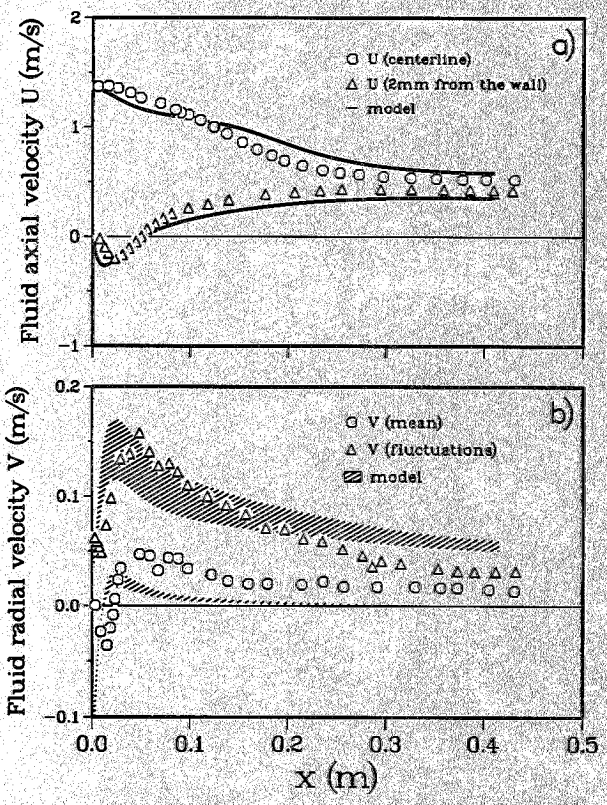

Figure 1(a) — Predictions and measurements of the mean axial fluid velocity for flow through a sudden expansion — test case 1.
Figure 1(b) — Predictions and measurements for the mean and fluctuating component of the radial fluid velocity, 2 mm from the wall, for flow through a sudden expansion — test case 1.

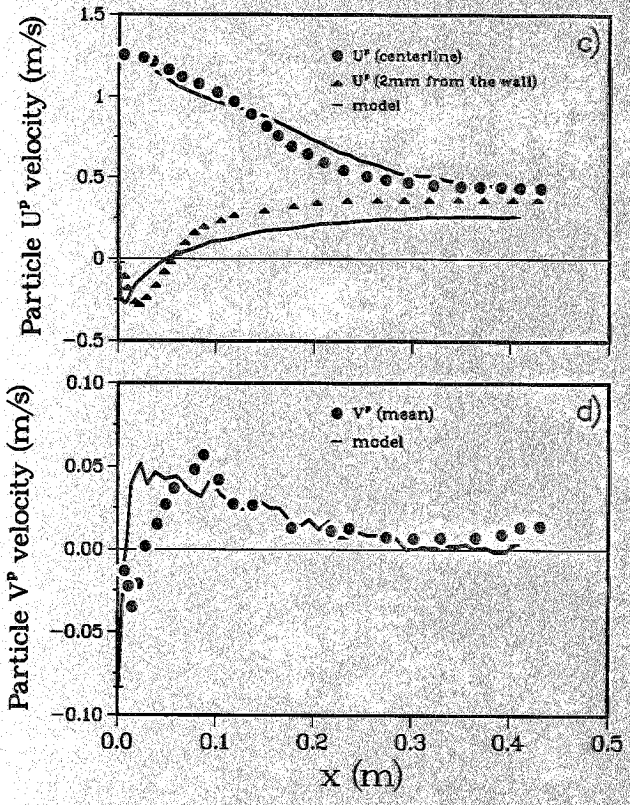

Figure 1(c) — Predictions and measurements of the particle mean axial velocity for flow through a sudden expansion — test case 1.
Figure 1(d) — Predictions and measurements of the particle mean radial velocity, 2 mm from the wall, for flow through a sudden expansion — test case 1. Measurements taken from Blatt et al. (1989).

the same authors. Test case parameters of importance for the present study are given in Table 1 along with some typical parameters of the numerical model.

Test case 1 — hydrodynamics

A number of hydrodynamic experimental two-phase flow studies employing Laser Doppler Anemometry (LDA) have appeared recently, most of them related to confined plane or axisymmetric jet flows (Tsuji et al., 1988; Mostafa et al., 1989). Ruck and Makiola (1988) have reported measurements of a dispersion of small (1–70 μm) particles in air flow over a plane backward-facing step also by using LDA. In the present study hydrodynamic measurements of Blatt et al. (1989) were used to verify the accuracy of the employed flow model. They have shown LDA measurements for flow of water carrying 1000 ppm of 800 μm diameter glass spheres through a sudden pipe expansion.

The measured and predicted decay of the mean fluid axial centerline velocity is shown in Figure 1a. Both curves have the same character with the maximum discrepancy (10%) being somewhat larger than for single-phase flow (Nesić and Postlethwaite, Part I, 1991). Predictions show somewhat faster spreading of the jet which is typical for the used model of turbulence. Further downstream higher values are obtained in the simulations. It is suspected that "migration" of particles towards the walls is higher in the predictions, yielding smaller concentrations of particles in the core, this causing lower drag and smaller deceleration of the fluid. The opposite effect is noticeable when measurements and predictions are compared in the near-wall region (Figure 1a). The axial velocity 2 mm from the wall is slightly underpredicted.

Figure 1b shows comparisons of predictions and measurements of the fluid radial velocity components, mean and fluctuating, 2 mm from the wall (in the buffer layer). As in LDA measurements the measuring volume is approximately 1 mm in diameter, and the gradients in the near wall region are very high, predictions near the wall are shown as a shaded area bordered with values obtained at 1.5 mm and 2.5 mm, from the wall. The predictions of the fluid fluctuating velocity show good agreement with the measured values, taking into account that the predictions show a space-averaged value, while the measurements present the radial component of the fluctuating velocity near the wall. The predicted asymptotic value is higher, as it is known that near the wall the axial component of the fluctuating velocity is larger than the radial, so the predicted space-averaged value is expected to be larger than the measured radial component. Predictions of mean fluid radial velocity show moderate agreement with the experiments.

Figure 1c shows the particle mean axial velocity at the centerline and 2 mm from the wall. In case of the centerline velocity, the agreement between the predictions and measured values is good. The near-wall values show larger discrepancies, although the character of the curve is captured with the predictions. The agreement for the near-wall particle mean radial velocity profiles shown in Figure 1d is similar. Milojević et al. (1986) reported similar problems in the near wall region when they simulated flow of a confined coaxial air jet loaded with glass spheres. One explanation is the inadequacy of the wall function approach in modelling two-phase flow, as particles interfere with the shape of the universal velocity profile. Also, near the wall due to the particle-wall interactions, interpretation of obtained particle parameters is quite complicated. Overall,

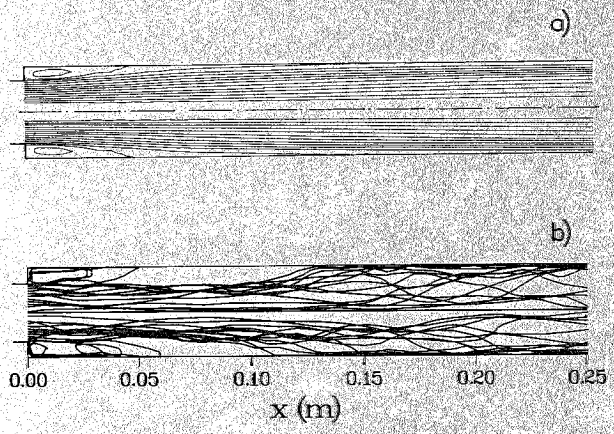

Figure 2 — (a) Predicted fluid flow streamlines — test case 1. (b) 30 of the 2000 predicted particle trajectories — test case 1.

we can consider the agreement of the predicted and measured hydrodynamic parameters of test case 1 satisfactory.

Test case 2 — Erosion

Stainless steel erosion measurements of Lotz and Postlethwaite (1990) for flow of a 2% vol. sand slurry through a sudden pipe expansion were used to test the two presented models of erosion. In order to calculate erosion rates information on particle-wall impact is needed: angles of impact, velocities and mass of impacting particles, along the pipe wall. In order to obtain a converged numerical solution, calculation of 2000 individual trajectories was performed. Predicted particle-wall impact parameters that are presented are average, overall impacts registered at a given location on the wall. Here, one of the important advantages of Lagrangian models for particle motion over Eulerian emerges, as all particle-wall parameters can be calculated directly by averaging, while Eulerian models, that treat particles as a "second fluid", require modelling.

Figure 2a shows the predicted fluid streamlines with the flow separation and reattachment and the large recirculation zone in the corner, and Figure 2b presents a small sample (30) of the calculated particle trajectories. The effect of turbulence on the stochastic nature of particle motion is clearly visible. It can be noticed that a small proportion of particles gets caught up in the recirculation zone, while the majority are carried toward the wall by the fluid.

Predicted average particle-wall impact parameters are shown in Figure 3. The average number of impacts (Figure 3a) varies from 2-20 $mm^{-2}\ s^{-1}$, which corresponds to an average impact mass of 0.2–2.5 $kg/m^2 \cdot s$. The maximum is moved downstream from the reattachment point and reflects the inertia of the particles, which do not "sense" the sudden expansion directly but rather through the drag force of the fluid. The average impact angle (Figure 3b) has a maximum (60°) close to the fluid reattachment point, which is to be expected, as this is the turn-around point for the particles that get caught up in the recirculation eddy. Further downstream the average angle of impact decreases and is about 5° in the region of a fully redeveloped turbulent pipe flow. This corresponds to the so called "sliding impacts" that create very little erosion. The curve of the average particle impact radial velocity (perpendicular to the wall), shown in Figure 3c, has a similar character, as the two are related directly. Maximum values of 0.8 m/s are above the critical velocity U_{cr} = 0.668 m/s determined by Bitter (1963), for

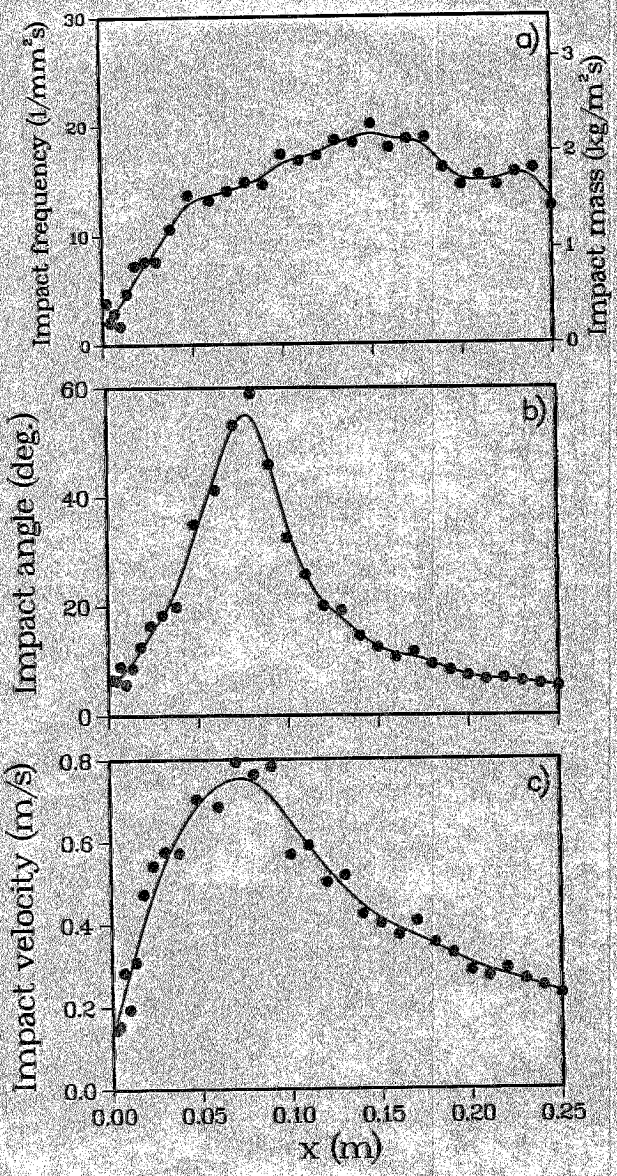

Figure 3 — (a) Average particle-wall impact frequency and impact mass — test case 2. (b) Average particle-wall impact angle — test case 2. (c) Average particle-wall impact velocity perpendicular to the wall - test case 2.

erosion of stainless steels. In the region of redeveloped turbulent flow, predicted average impact velocity of the sliding impacts is lower than this limit, which does not mean that there are no individual impacts that exceed the limit. This can be seen on Figure 4b where a small but finite rate of erosion was predicted despite the average velocity being smaller than critical.

Both the original Finnie (1960) Equations (7) and (8) and Bergevin's (1984) modified Equations (9), (10) were incorporated into the LSD particle motion model. Predictions obtained with Finnie's equations (Figure 4a) are an order of magnitude higher than the measured values of Lotz and Postlethwaite (1990). If the value of the arbitrary constant of c = 0.5 was used as suggested by Finnie (1960), the predicted values would still be too high. The other problem is the shape of the predicted erosion profile, which does not resemble the character of the measured erosion profile. The local minimum close to the reattachment point corresponds to high impact angles, where this model is known to underpredict erosion. Our conclusion was that Finnie's equations,

TABLE 1
Important Geometric, Hydrodynamic and Numerical Parameters

	Test case 1	Test case 2	Test case 3
Inlet diameter (mm)	26	21	21
Outlet diameter (mm)	40	42	42
Length (mm)	420	500	500
Inlet fluid velocity (m/s)	1.14	13.2	13.2
Outlet fluid velocity (m/s)	0.48	3.3	3.3
Inlet Reynolds number	37000	340000	340000
Outlet Reynolds number	24000	170000	170000
Particle diameter (μm)	800	430	430
Inlet particle velocity (m/s)	1.08	13.1	13.1
Particle concentration (%vol.)	0.1	2	2
Number of x grid points	48	58	58
Number of y grid points	12	14	14
Number of particle trajectories	2000	2000	2000
Number of iterations	292	351	351
Total error of predictions (%)	1	1	1
VAX 6320 CPU time (min)	113	152	152

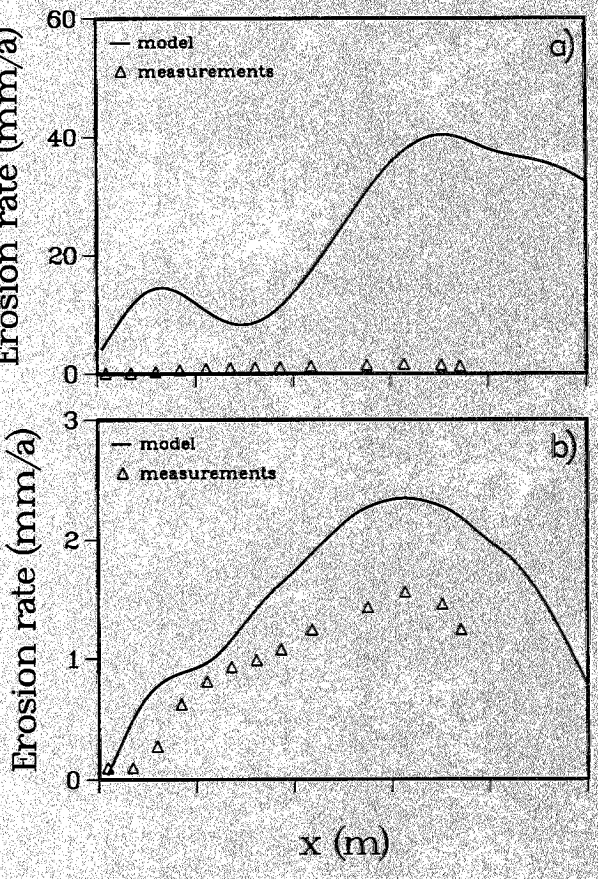

Figure 4 — Erosion rate measurements and predictions made with Finnie's equations — test case 2. (b) Erosion rate measurements and predictions made with Bergevin's equations — test case 2 Measurements taken from Lotz and Postlethwaite (1990).

even tuned with the c constant, still do not give satisfactory predictions. The reason is that the initial assumption inherent to the model, that every impact creates a damage, which is known to be wrong, is only masked but not eliminated with the use of the constant c.

On the other hand predictions obtained with Bergevin's (1984) Equations (Figure 4b), have the same order of magnitude and character as the measured profile of erosion. This suggests that using Bitter's (1963) concept of critical velocity U_{cr}, is correct. His value given for stainless steel ($U_{cr} = 0.668$), used directly in our model, gave good predictions. Also, there is no need for the arbitrary constant c, which adds to the generality of the model. The shortcomings of Finnie's (1960) model related to high impact angles have not been eliminated in this model completely, but are of much less significance. This could be improved by using an additive correction for high impact angles as suggested by Zeisel and Durst (1990). Some scattering of the predicted points, not shown on Figure 4, was obtained due to the statistical procedure by which the results were obtained. The number of trajectories (2000) used, should be increased to smooth out the predictions, but this was impractical on the computer used, with respect to the already very long computation time (Table 1).

TEST CASE 3 — EROSION-CORROSION

Measurements of Lotz and Postlethwaite (1990), with flow of an oxygen saturated 2% sand slurry, through a sudden pipe expansion, were used to study the effect of hydrodynamics on erosion–corrosion. In their analysis the authors suggested that nearly all the formed rust was removed by the erosive action of the particles. As the corrosion rate was oxygen-mass transfer controlled, in absence of a rust

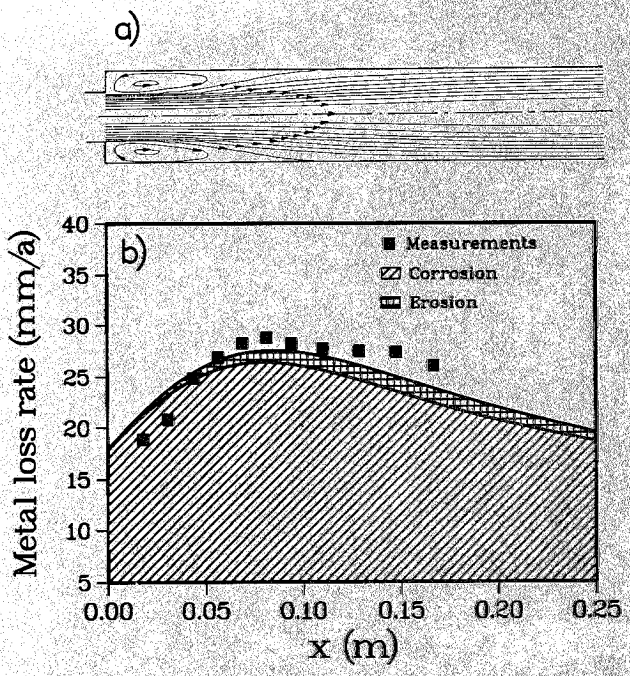

Figure 5 — (a) Predicted fluid flow streamlines — test case 3, (b) Measured rates of erosion–corrosion (Lotz and Postlethwaite, 1990) and predicted rates of corrosion and erosion of the base metal — test case 3.

layer the only resistance for mass transfer was in the liquid boundary layer.

To predict the mass transfer resistance of the boundary layer we can use the correlation for the Sherwood number, determined by Nešić and Postlethwaite, Part I (1991). The predicted level of turbulent fluctuations in the buffer layer, for this test case, 100 mm downstream of the expansion, where measured erosion–corrosion rate reaches its maximum, is 0.43 m/s. The correlation yields a Sherwood number Sh = 4882, when corrected for the actual Schmidt number ratio. This corresponds to a mass transfer coefficient of 2.72×10^{-4} m/s, and finally an increase by a factor 1.8, to account for the effect of roughness (Postlethwaite and Lotz, 1988), gives a predicted oxygen-mass transfer coefficient $k_f = 4.9 \times 10^{-4}$ m/s. Converted into a metal loss rate this is 25 mm/a. When we add the erosion component of the bare metal determined by the erosion model with Bergevin's (1984) Equations (9) and (10), of 1.5 mm/a, the final predicted metal loss rate is 26.5 mm/a. The measured rate of metal loss in the erosion–corrosion experiments (Figure 5b) was 27 mm/a. The agreement with the predicted value is very good.

Further downstream the flow returns to a fully developed turbulent pipe flow, and going through the same calculation procedure we can predict a corrosion rate of 19.2 mm/a and an erosion rate of 0.8 mm/a. The total metal loss rate of 20 mm/a is close to the asymptotic value suggested by the experimental curve. A corrosion rate of 23 mm/a is obtained, if the experimental correlation of Postlethwaite and Lotz (1988) for mass transfer at rough surfaces in pipes carrying slurries, is used instead, which is slightly higher.

Comparison of the overall predicted rate of metal loss (corrosion plus erosion) is in good agreement with the measured erosion–corrosion rate (Figure 5b). It is clear that the dominant mode of metal loss is corrosion, with the sand removing the protective rust film. The rate of erosion of the base metal was an order of magnitude smaller than the rate of corrosion. The models of flow and erosion–corrosion used, were successful in predicting the overall rate of metal loss.

Conclusions

1. The predictions made with the two-phase flow model, which includes a $\mathbf{k} - \epsilon$ model of turbulence, accompanied with a Lagrangian Stochastic Deterministic (LSD) model for particle motion, have shown an overall good agreement with the LDA measurements, for flow of water carrying 1000 ppm of 800 μm glass spheres, through a sudden pipe expansion. Some discrepancies obtained for the near-wall region are ascribed to the difficulties in measurements close to the walls, and to the inadequacy of the applied wall function approach, for modelling near-wall two-phase flow.
2. An erosion model based on original and modified Finnie's (1960) erosion equations, was incorporated into the (LSD) model for particle motion. Predictions of erosion rates were in good agreement with the stainless steel erosion measurements, for a 2% water/sand slurry flow through a sudden expansion, when modified equations were used. The model of erosion used, requires as input only the yield strength of the eroded material and the critical velocity for plastic deformation, as defined by Bitter (1963). Both are easy to obtain experimentally.
3. Predictions of metal loss by erosion–corrosion were made and compared with erosion–corrosion measurements for flow of oxygen saturated 1% water/sand slurry through a sudden pipe expansion. It was found that the dominant mode of metal loss is corrosion, with the sand removing the protective rust film. Rate of erosion of the base metal was an order of magnitude smaller than the rate of corrosion. The model of flow and erosion–corrosion used were very successful in predicting the overall pattern and rate of metal loss.

Nomenclature

A'	= projected area for the particle, m^2
c	= constant
C_D	= drag coefficient
d'	= particle diameter, m
D	= diffusion coefficient, m^2/s
f'	= drag coefficient for flow around a sphere
F	= force, N
$\mathbf{k}$	= kinetic energy of turbulence, m^2/s^2
L_t	= length scale of turbulence, m
m'	= particle mass, kg
p	= yield strength, Pa
Q	= metal loss rate, m^3
Re	= Reynolds number, $Re = ul/\nu$
Sc	= Schmidt number, $Sc = \nu/D$
t	= time, s
T_L	= Lagrangian integral time scale, s
u, v, w	= components of the fluctuation velocity vector, m/s
U, V, W	= components of mean velocity vector, m/s
$\tilde{u}, \tilde{v}, \tilde{w}$	= components of the instantaneous velocity vector, m/s
$u'; v'; w'$	= means of the components of fluctuation velocity (RMS), m/s
$\tilde{u}_R^p$	= particle reflection velocity, m/s
U_{cr}	= critical velocity for plastic deformation, m/s
V_r	= mean radial velocity, m/s
$\vec{V}$	= velocity vector, m/s
x	= axial coordinate, m

Greek letters

α = impact angle
ϵ = dissipation rate of kinetic energy of turbulence, m^2/s^3
Ψ_R = particle-wall reflection coefficient
ρ = fluid, density, kg/m^3

Superscripts

p = refers to particles
$\sim$ = stands for instantaneous value

References

Bergevin, K., "Effect of Slurry Velocity on the Mechanical and Electrochemical Components of Erosion–Corrosion in Vertical Pipes", M.Sc. thesis, Univ. of Saskatchewan, Saskatoon (1984).

Bitter, J. G. A., "A Study of Erosion Phenomena — Part I", Wear **6**, 5–21 (1963).

Blatt, W. and E. Heitz, "Hydromechanical Measurements for Erosion–Corrosion", Conf. Corrosion/90, paper 25, NACE, Houston, TX (1990).

Blatt, W., T. Kohley, U. Lotz and E. Heitz, "The Influence of Hydrodynamics on Erosion–Corrosion in Two-Phase Liquid/Particle Flow", Corrosion, **45**, 793–803 (1989).

Durst, F., D. Milojević and B. Schonung, "Eulerian and Lagrangian Predictions of Particulate Two-Phase Flows: A Numerical Study", Appl. Math. Model. **8**, 101–115 (1984).

Finnie, I., "Erosion of Surfaces by Solid Particles", Wear **3**, 87–103 (1960).

Glaeser, W., "Erosion–Corrosion Cavitation and Fretting, Forms of Corrosion Recognition and Prevention", C. P. Dillon, Ed., NACE, Houston, TX (1982).

Launder, B. E. and D. B. Spalding, "The Numerical Computation of Turbulent Flows", Comp. Meth. Appl. Mech. Eng. **3**, 269–289 (1974).

Lotz, U. and J. Postlethwaite, "Erosion–Corrosion in Disturbed Two Phase Liquid/Particle Flow", Corrosion Sc. **30**, 95–106 (1990).

Milojević, D., T. Borner and F. Durst, "Prediction of Turbulent Gas-Particle Flow Measurement in a Plain Confined Jet", World Congress Particle Technology, Part IV, Partikel Technologie Nurnberg, Nurnberg, W. Germany (1986).

Mostafa, A. A., H. C. Mongia, V. G. McDonell and G. S. Samuelsen, "Evolution of Particle Laden Jet Flows: A Theoretical and Experimental Study", AIAA J. **27**, 167–183 (1989).

Nešić, S. and J. Postlethwaite, "Erosion–Corrosion Under Disturbed Flow Conditions in Slurry Pipelines", Corrosion/90, paper 26, NACE, Houston, TX (1990).

Nesić, S. and J. Postlethwaite, "Hydrodynamics of Disturbed Flow and Erosion–Corrosion, Part I — A Single-Phase Flow Study", Can. J. Chem. Eng. **69**, xxx–xxx (1991).

Postlethwaite, J., M. H. Dobbin and K. Bergevin, "The Role of Oxygen Mass Transfer in the Erosion–Corrosion of Slurry Pipelines", Corrosion **42**, 514–521 (1986).

Postlethwaite, J. and U. Lotz, "Mass Transfer at Erosion–Corrosion Roughened Surfaces", Can. J. Chem. Eng. **66**, 75–78 (1988).

Pourahmadi, F. and J. A. C. Humphrey, "Modelling Solid-Fluid Turbulent Flows With Application to Predicting Erosive Wear", Physico-Chemial Hydrodynamics **4**, 191–219 (1983).

Ruck, B. and B. Makiola, "Particle Dispersion in a Single-Sided Backward-Facing Step Flow", Int. J. Multiphase Flow **14**, 787–800 (1988).

Tsuji, Y., Y. Morikawa, T. Tanaka, K. Karimine and S. Nishida, "Measurement of an Axisymmetric Jet Laden With Coarse Particles", Int. J. Multiphase Flow **14**, 565–574 (1988).

Zeisel, H. and F. Durst, "Computations of Erosion–Corrosion Processes in Separated Two-Phase Flows", Conf. Corrosion/90, paper No. 29, NACE, Houston, TX (1990).

Manuscript received July 6, 1990; revised manuscript received January 9, 1991; accepted for publication January 18, 1991.